PCCP

Accepted Manuscript

ROYAL SOCIETY OF CHEMISTRY

www.rsc.org/pccp

PCCP

RSCPublishing

ARTICLE

Pressure-induced molten globule state of human acetylcholinesterase: Structural and dynamical changes monitored by neutron scattering

Cite this: DOI: 10.1039/x0xx00000x

Received ooth January 2012,
Accepted ooth January 2012

DOI: 10.1039/x0xx00000x

www.rsc.org/

J. Marion[a,b,†], M. Trovaslet[a,c,†], N. Martinez[a,b], P. Masson[a,d], R. Schweins[b], F. Nachon[a,b], M. Trapp[e,f], J. Peters[a,b,*]

We used small-angle neutron scattering (SANS) to study the effects of high hydrostatic pressure on the structure of human acetylcholinesterase (hAChE). At atmospheric pressure, our SANS results obtained on D11 at ILL (Grenoble, France) give a radius of gyration close to that one calculated for a mixture of monomers, dimers and tetramers of the enzyme, suggesting a good agreement between hAChE crystal structure and its conformation in solution. Applying high pressure to the sample we found a global compression of about 11% of the enzyme up to a pressure of 900 bar and then again an extension up to 2.1 kbar indicating unfolding of the tertiary structure due to a molten globule (MG) state. On the other hand, we studied the influence of pressure up to 6 kbar on the dynamics of this enzyme, on the backscattering spectrometer IN13 at ILL. For the first time, we used elastic incoherent neutron scattering (EINS) to probe the differences between hAChE in its folded state (N), its high-pressure induced MG state and its unfolded state (U). Especially around the MG state at 1750 bar we found a significant increase in the dynamics, indicating a partial unfolding. A four-step-model is suggested to describe the changes in the protein.

1. Introduction

One of the most intriguing goals of high-pressure studies is the characterization of folding and unfolding processes of proteins[1]. In fact, pressure is generally considered as a potential denaturant of biomolecules, with the great advantage that it affects mainly the volume of the system, whereas temperature denaturation involves changes in both the volume and the thermal energy[2]. Moreover, while pressure denaturation of proteins is generally reversible up to pressure values well above those existing on Earth's biosphere (about 1 kbar at the bottom of the deepest trench of the ocean, 1 bar = 0.1 MPa), temperature denaturation of proteins appears often more violent in its influence on the tertiary and secondary structures and may result in irreversible aggregation, and chemical deterioration.

The classical Lumry-Eyring's two-state model seems to be insufficient to describe in detail protein folding or unfolding processes.[3,4] Under certain mild conditions, at least one intermediate state between the fully folded native state (N) and the fully unfolded state (U) may exist. This intermediate is named molten globule state (MG). Its main common properties are (1) the presence of a significant amount of secondary structure, (2) the absence of most of the specific tertiary structure produced by the tight packing of side chains, (3) compactness of the protein molecule that swells with a radius of gyration 10%–30% larger than that of the native state, and (4) the presence of a loosely packed hydrophobic core that increases the hydrophobic surface accessible to solvent.[5-7]

The present study is devoted to the MG transition of human acetylcholinesterase. This enzyme has a paramount physiological importance because it terminates the action of the neurotransmitter acetylcholine in central nervous system, peripheral nervous system ganglia, and at neuromuscular junctions.[8-10] Numerous MG states have already been described during thermal, chemical and/or high-pressure-induced unfolding of cholinesterases (*Torpedo californica* acetylcholinesterase, human butyrylcholinesterase, human acetylcholinesterase)[11-15] and of other proteins.[16-19] During high-pressure denaturation of human acetylcholinesterase (hAChE), the enzyme that plays a central role in the cholinergic system by rapidly hydrolyzing the neurotransmitter acetylcholine, several enzyme conformational and functional alterations were observed. These pressure-induced changes have already proved the presence of a MG state between 1 and 2 kbar.[15] Characteristics of this pressure-induced MG intermediate have been studied intensively (ANS binding, electrophoresis mobility under pressure, hydrodynamic volume, activity) by these authors. Though MGs are unstable transient

states, little is known about the dynamics of these partially folded states. The molecular dynamics which can be probed on the time scales accessible by incoherent neutron scattering (a few ps up to a few ns) corresponds to diffusional processes. It was established over the last decades that protein dynamics is associated to its conformational flexibility[20,21], which is mandatory for enzyme catalysis and molecular activity[22], shortly for its function. However, most proteins are only functional in their folded state, against being non-functional in the unfolded state. MGs are intermediate states which lost part of their structure, but not necessarily their activity which can be modulated considerably. Therefore supposing a dynamics-function-activity relation, knowledge of the dynamics of MG states would be highly important to characterize such modulations.

In the case of cholinesterases no information is available on the dynamics of MGs so far. Yet, MG transition of these enzymes can occur under standard conditions of pressure and temperature upon binding of specific ligands or reactive chemicals[11,13]. Also, a naturally occurring point mutation has been found to lead to a cholinesterase variant that is in a conformational state similar to MG.[23] Therefore, it was of great interest to access a method capable of providing information on the dynamics of acetylcholinesterase MG transition. Our study was performed under pressure in the range 10^{-3} to 6 kbar.

For this purpose, incoherent neutron scattering offers a method to study molecular dynamics with the advantage of measuring average atomic motions within a given length-time window, which depends on the specific resolution parameters of the instrument. The incoherent neutron scattering intensity is dominated by the signal arising from hydrogen. This is due to the hydrogen incoherent scattering cross section, which is one order of magnitude larger than that of all other elements usually occurring in biological matter, and also of its isotope deuterium.[24] The technique thus probes local molecular dynamics, arising mainly from amino acids sidechains, averaged over the whole macromolecule. hAChE contains a high proportion of hydrogen, 4673 of a total of 9470 atoms. The incoherent cross section of the hydrogen atoms thus corresponds to 99.8% of the total incoherent cross section and to 92.6% of the total scattering of the sample (without the D_2O hydration layer). As we are measuring in solution, heavy water represents about 90% of the total volume, but the contribution to the incoherent scattering remains negligible.

There have already been extensive applications of neutron scattering to dynamics' studies of several different biological systems.[21,25] However, compared to other techniques, such studies are still scarce, mainly because of the need of a relatively high sample amount (about 100 – 200 mg of pure proteins) to get a reasonable signal-to-noise ratio and the restricted availability of intense neutron sources. This is all the more true when combining neutron scattering with high pressure, as high pressure cells adapted to these scattering techniques became only recently available.[26-29]

Thus, the main challenge of our study was to better characterize the structure and dynamics of MG state formed during high-pressure-induced denaturation of hAChE. Firstly, from SANS experiments, the overall conformation of hAChE was observed up to 2.1 kbar (the highest possible value with the present high hydrostatic pressure (HHP) equipment for SANS at the ILL) by measuring its radius of gyration. Unfortunately, higher pressure could currently not be reached, therefore no structural information was accessible about the unfolded state. Secondly, we used EINS to follow the high-pressure-induced modifications in the dynamics of hAChE, up to 6 kbar, the maximum accessible with the corresponding HHP cell.

2. Materials and methods

2.1 Sample preparation

Production and purification of the full-length recombinant hAChE were executed as described previously in [30]. An additional size-exclusion chromatography on Superdex-200 in ammonium acetate buffer (25 mM, pH 7.4) allowed the removal of minor aggregated proteins and desalting. The stock solution of enzyme was then extensively dialyzed against deuterated ammonium acetate buffer (25 mM, pD is around 7 so the pH is about 6.6,[31] because heavy water is less dissociated and a weaker acid than light water) until almost all accessible hydrogen atoms were exchanged against deuterium to avoid a significant signal contribution from the surrounding buffer.

For SANS experiments, 3 ml of a 0.4 mg/ml protein solution was prepared by dilution of the enzyme stock solution in a deuterated ammonium acetate buffer 25mM with a pD close to 7 (corresponding to a pH of 6.6). The protein concentration was determined from its absorbance at 280 nm using a molar extinction coefficient of 1.7 for 1 mg/ml of protein.[32]

For EINS experiments, after a 24h-lyophilisation step of the enzyme stock solution, about 200 mg of protein powder was dried over P_2O_5 and hydrated by D_2O vapor exchange. For this experiment, the hydration was adjusted to be about 2 g D_2O/g protein. Due to this very high degree of hydration, a gel was formed which was loaded into the high pressure cell. The sample volume was further filled up with D_2O to permit a uniform distribution of the applied pressure. The sample volume was evaluated to be about 9.6% of the total volume.

2.2 Nondenaturating 10% polyacrylamide gel electrophoresis

Before and after the SANS experiment, protein analysis was carried out by native electrophoresis on 10% acrylamide/bis-acrylamide gels (Mini-Protean Precast Gels, Biorad). Electrophoresis buffer was Tris/glycine (41mM/0.533M) pH 8.4. All samples were diluted in running buffer containing sucrose (40%) and bromophenol blue as a tracking dye (0.05%) in order to obtain a correct protein concentration (some µg protein per lane). All samples were loaded twice onto the gel and, after electrophoresis, the gel was cut into two parts: the first one was stained with Coomassie Brilliant Blue (lanes 1 and 2) and the second one was stained for cholinesterase activity according to the method of Karnovsky and Roots[33] (lanes 3 and 4). Acetylthiocholine (1mM) was then used as substrate and the gel was immersed in the reaction mixture for a few minutes at room temperature. AChE activity bands appeared as red-brown bands.

2.3 Small angle neutron scattering experiment

SANS experiments were performed on D11 (ILL, Grenoble, France)[34] in order to observe the structural conformational

changes induced by pressure. For this work, we carried out measurements using two sample-detector distances, e. g. 2.5 and 10 m, with collimation distances of 5.5m and 10.5m respectively. The neutron wavelength was set to $\lambda = 4.6$ Å and a wavelength resolution $\Delta\lambda/\lambda$ of 9%. The magnitude of the scattering vector Q was ranging from 0.0086 to 0.3432 Å^{-1}. The sample was illuminated with an 8mm diameter neutron beam. Scattered neutrons were detected with a position-sensitive ^{3}He detector which is composed of an active area of 128x128 pixels with a size of 7.5x7.5mm each. All data are normalized to absolute intensities in units of 1/cm by measuring H_2O of 1mm path-length as secondary calibration standard, which is cross-calibrated against H/D polymer blends; the wavelength-dependent effective differential cross section of H_2O for the D11 detector is $d\Sigma/d\Omega = 0.903$ cm^{-1}. Data were recorded at ambient pressure both in a Hellma cell and in the high pressure cell to validate the equipment. In the Electronic Supplementary Information (ESI), figure 1 represents these two curves as Kratky plots.[35]

Data reduction was done using the "SANS treatment macro" of the LAMP software developed at the ILL. First, the two-dimensional data are reduced, as first step an electronic background (measurement of a beam blocker like Cadmium) was taken off of all data. Also, data were transmission-corrected and the empty pressure cell has been subtracted. As the scattering intensities were isotropic, a radial averaging of the two-dimensional data was performed with respect to the centre of the incoming neutron beam, yielding the presented one-dimensional scattering curves. Last, the normalized solvent scattering curve has been subtracted from the normalized sample scattering curves. The solvent has been measured in the pressure cell and as a function of pressure, too. As the intensities did not differ as a function of pressure, the different solvent scattering curves were averaged to minimize the intensity error bars and the obtained scattering curve was subtracted from all sample scattering curves. The incoherent background was not subtracted, but taken into account through a fitting parameter within the Guinier fits that were done using SASVIEW.

The sample was loaded in the SANS pressure cell (described in [29]). The applied pressure ranged from 1 bar to 2.1 kbar. The pressure was then released with a velocity of about 1 kbar/min and the measurement was started again after 5 minutes.

The Guinier approximation[36] permits to extract the radius of gyration R_G, which is a measure for the moment of inertia, thus the dimensions of an object, through:

$$I(\vec{Q}) \approx \bar{b}^2 V^2 e^{-\frac{Q^2 R_G^2}{3}}, \quad (1)$$

where $\bar{b}$ is the average scattering length and V the volume of the object. The well-known Guinier approximation holds for small values of momentum transfer Q, which corresponds to the initial linear slope of the scattering curve in the representation of lnI vs. Q^2.[37] The intensity I_0 at $Q \rightarrow 0$ is thus proportional to V^2.

2.4 Elastic incoherent neutron scattering experiment

The experiment was performed on the backscattering spectrometer IN13 (ILL, Grenoble, France).[38] IN13 was configured with a 2.23 Å incoming neutron wavelength and 0.2 to 4.9 Å^{-1} momentum transfers, corresponding to an energy resolution of 8 μeV and allowing to probe local motions up to 100 ps. We used the Gaussian approximation[39]

$$I(Q,0 \pm \Delta E) \approx \exp\left(-\frac{1}{3}\langle u^2 \rangle Q^2\right) \quad (2)$$

in order to treat the data in a 0.8-2.7 Å^{-1} Q-range and to extract the atomic mean square displacements (MSD) $\langle u^2 \rangle$ from the neutron intensities I. Similar to the Guinier approximation, it is valid for small Q-values, e.g. when $\sqrt{\langle u^2 \rangle Q^2} \leq \sqrt{2}$. ΔE designates here the instrumental energy resolution.

To obtain the intensities scattered by the sample only for the SANS and EINS experiments, the scattering from the empty sample holder with the buffer (D_2O) was subtracted. The data were normalized to the totally incoherent scatterer Vanadium and absorption corrections based on the formula of Paalman-Pings[40] were applied. For SANS, 1mm thick H_2O was used as secondary calibration standard (cross-calibrated against H/D polymer blends); the differential scattering cross section of H_2O for the D11 detector at 4.6 Å is 0.908 cm^{-1}. The complete data reduction for SANS and EINS was carried out using the LAMP software available at ILL.[41] Additional linear corrections were made assuming that the compressibility of heavy water results in a 20% volume decrease when going from 1 to 6000 bar. We neglected, however, the protein compressibility due to the fact that hAChE represented only 9.6% of the total volume, for a density of 1.40 (g cm^{-3})[42] and that typical compressibilities of globular proteins in solution would give rise to linear compression of about 3%, only.[43] The illuminated sample area was 10 x 21 mm^2 for the EINS experiments and a circle of 8mm diameter for the SANS experiments. With raising pressure, more and more proteins were thus pushed into the beam due to the volume reduction and led to a slight increase of the scattered intensity, which was then renormalized. Calculations of the absorption coefficients were made using the program DAVE[44] in order to verify that they do not change with the Q value. Furthermore we evaluated with the same software multiple scattering effects; they were negligibly small in the present case.

3. Results and discussion

3.1 SANS experiments

Figure 1 shows SANS curves of hAChE measured on D11 at 1 bar, 300 bar, 2100 bar and again at 1 bar. The curves at 600, 900, 1200 and 1800 bar were all close to the 2100 bar data and are not shown here. After releasing the pressure, the intensity was not relaxing exactly to the starting values.

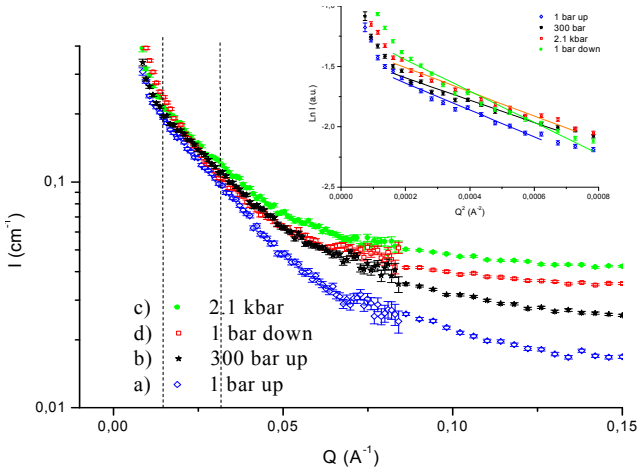

Fig. 1: Neutron intensity *vs.* the scattering vector magnitude *Q* measured at (a) 1 bar (in blue, open diamond), (b) 300 bar (in black, filled star), (c) 2.1 kbar (in green, filled circle) and (d) after pressure release (in red, open square). The insert shows the corresponding Guinier plots. The dashed vertical lines highlight the Q-range used the extract them.

We extracted radii of gyration and the intensities I_0 (see figure 2) through Guinier plots of ln(I) against Q^2. For that we used Q-ranges from 0.012 to at the most 0.029 $Å^{-1}$ to stay below $R_G*Q < 1.45$.

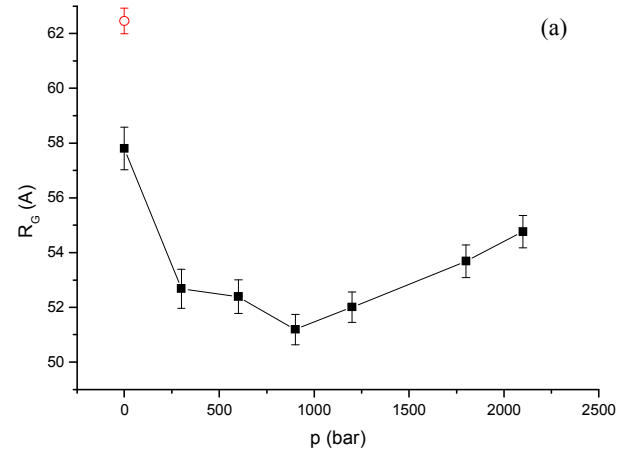

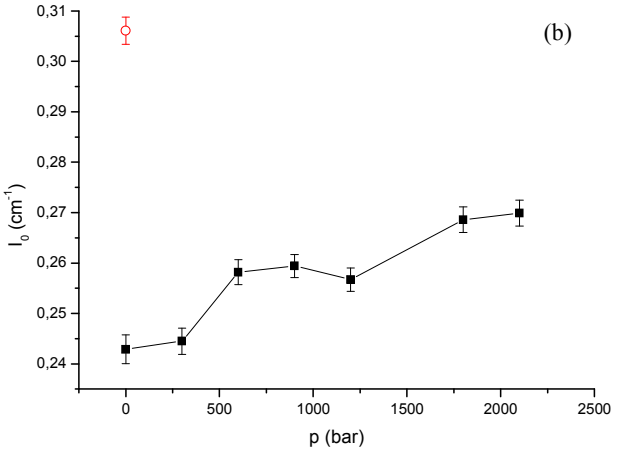

Fig. 2: (a) The radius of gyration and (b) intensity at Q → 0 vs. applied pressure. The red point (open circle) corresponds to the values after releasing pressure.

hAChE is a globular protein of a molecular weight of 67.8 kDa. The theoretical value for R_G of the hAChE dimer crystal structure could be estimated by analyzing the three-dimensional truncated hAChE crystallographic data 3LII[45] or 4EY4[46] with the CRYSON program.[47] This led to a R_G = 37.63 or 38.15 Å for the dry enzyme (respectively for 3LII and 4EY4) and to R_G = 45.72 or 46.27 Å for the same proteins including a 3-Å-thick hydration shell. We therefore estimated the total increase of the radius due to the hydration shell by the difference of the two values to be about 7 Å. The electrophoresis (see figure 3) permitted to determine, that in the present case we have a mixture of monomers, dimers and tetramers. Their radii of gyration were calculated to be 26.9, 45.7 and 53.7 Å, respectively, assuming that $\left(R_G^2\right)_{dimer} = 2\left(R_G^2\right)_{monomer}$ and $\left(R_G^2\right)_{tetramer} = 2\left(R_G^2\right)_{dimer}$ and adding the hydration shell again at the end. Finally, we evaluated the average radius of gyration of the mixture according to[48]

$$\left\langle R_G^2 \right\rangle = \sum_i M_i c_i (R_G^2)_i \Big/ \sum_i M_i c_i \quad , \qquad (3)$$

where M_i are the molecular weights and c_i the concentrations of the three species. According to figure 3 we estimated 10% of monomers, 60% of dimers and 30% of tetramers yielding a value of 53.6 Å when including the hydration shell. This result is rather close to the experimental one of 57.8 Å, when considering that the estimate of the different concentrations is very rough. We neglected willingly the aggregates, because we ignore their composition and therefore their radius of hydration, but taking them into account would still increase the average radius of gyration and bring it in even closer agreement with the experimental value.

The R_G of hAChE decreases first for pressures up to 900 bar (R_G = (57.8 ±0.8) Å at atmospheric pressure vs. R_G = (51.2 ± 0.6) Å around 900 bar, corresponding to a maximum decrease of about 11 %). The global compression of a few per cent is thus rather small, but because $V = 4\pi\ (5/3)^{3/2} R^3_G/3$ for a spherical protein, a small change in the radius (dR_G) can correspond to a significant change in volume $dV \approx 27\ R^2_G.dR_G$. It could have been the consequence of a dissociation of the oligomers, but Clery-Barraud et al. investigated cholinesterases under high pressure by electrophoresis[14,15] and never found any indication for such effects. Volume reduction is indeed expected under pressure application according to Le Chatelier's principle, but the radius rises again above 900 bar and this up to 2100 bar (by about 7 %), the highest pressure value we could reach with the pressure equipment actually available on D11. We relate the increase in size to a signature of the MG state which should be located around 1750 bar according to [15] and correspond to a partial unfolding.

We did furthermore SANS data analysis through a Kratky plot, representing $I*Q^2$ as a function of Q[35], after subtraction of the incoherent background (see figure 2 of the Electronic Supplementary Information ESI). The results show that the chosen range for the Guinier plots corresponds to a range where the intensities have very small error bars, even after subtraction of the incoherent background. At ambient pressure, the Kratky plot resembles a bell shaped profile, as expected for a globular protein. At 2.1 kbar the points at high Q values increase slightly bringing them closer to a plateau shaped profile when the

protein presumably starts to unfold. However, the precision of our data does not permit further exploitation and there is no real gain in information from this kind of data evaluation.

Activity measurements carried out before and after the high-pressure SANS experiment suggest that pressure-induced changes are mainly reversible in the tested pressure range. To confirm this result, protein analysis was carried out by native electrophoresis on T = 10% acrylamide/bis-acrylamide gels (Mini-Protean Precast Gels from Biorad) (see figure 3). Proteins were revealed by Coomassie Brilliant Blue staining (lanes 1 and 2) and the Karnovsky and Roots method[33] allowed us to detect cholinesterase activity (lanes 3 and 4). The native electrophoresis indicated that both initial and high-pressure treated hAChE preparations contained active monomer, dimer, tetramer and aggregates. The main observed difference was the pressure-induced formation of more aggregates after high-pressure treatment. As they were active, they were not denatured and their 3D-structure was not disturbed. This finding is in agreement with figure 2, which shows much higher values for the radius of gyration and I_0 after pressure release. The SANS scattering curves shown in Fig. 1 are obtained after subtraction of an averaged buffer intensity. All data are fully reduced, i.e. put on an absolute scale according to well-known and internationally agreed SANS data reduction procedures. The normalized buffer intensities were showing slight variations, but no pressure dependence (as to be expected). Therefore, the buffer measurements were averaged to gain in statistical accuracy. The remaining plateau at high Q is therefore caused by the incoherent scattering contribution of the proteins in solution. This does not contain any information on the structure of the proteins, it is only related to the total mass concentration of protein in solution (regardless of the fractions of mono-, di-, tetramers and clusters). Radii of gyration were obtained from the initial part of the scattering curves only, as stated above up to a Q of 0.029 $Å^{-1}$ to stay below $R_G*Q < 1.45$.

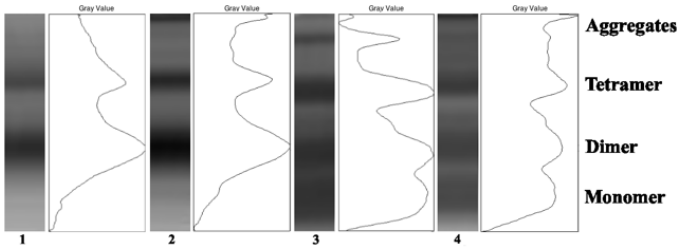

Fig. 3: Native electrophoresis and densitometry profiles obtained with from protein samples before (lanes 1 and 3) and after (lanes 2 and 4) pressure experiment. Samples were loaded twice onto the gel and after electrophoresis, the gel was cut into two parts: the first one was stained with Coomassie Brilliant Blue (lanes 1 and 2) and the second one was stained for cholinesterase activity according to the method of Karnovsky and Roots[33] (lanes 3 and 4).

3.2 EINS experiments

Figure 4 shows MSD of hAChE measured on IN13 as a function of pressure extracted from the Q-domain of 0.8 $Å^{-1}$ < Q < 2.7 $Å^{-1}$, corresponding to amplitudes between 2.3 and 8 Å. Water dynamics appears mainly at the smallest Q-values, which were excluded here from the data analysis. The dynamics taken into account corresponds therefore mainly to internal motions, global motions of the protein setting in at longer times (around 1 ns), although small contributions from such movements being not excluded as discussed in more detail in reference [49].

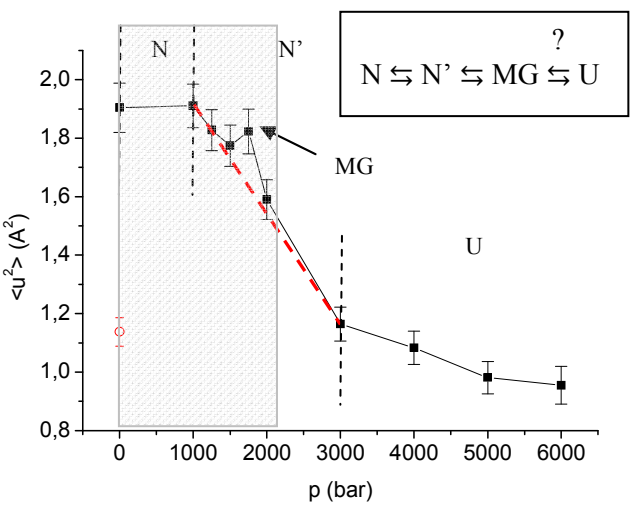

Fig. 4: Mean square displacement of hAChE, measured on IN13, at different pressures up to 6 kbar. The red point (open circle) corresponds to the MSD after releasing pressure. The red dashed line is guidance to the eye to illustrate the straight slope of this part of the curve. The dashed region corresponds to the pressure domain covered by the SANS measurement. The sketch on the right side illustrates the 4-step-model, N being the native, N' the transitional intermediates, MG the molten globule and U the unfolded state.

As already observed in EINS experiments carried out with other proteins under pressure (lysozyme[50], trypsin and β-lactoglobulin[51], for example), we monitored a global reduction in protein fluctuations suggesting a loss of protein mobility. This effect cannot be attributed to oligomerization, because EINS is not sensitive to it in the time range of about 100 ps accessible here as discussed in [30]. Almost no variation was visible up to 1 kbar (native state N), then a pronounced change in the MSD values (more than 50% variation) occurred in the low-pressure range tested (ensemble of transitional intermediate states N', up to 3 kbar). At 1750 bar (exactly in the range of pressure where the MG state of hAChE has previously been described[15], but shifted by about 200-300 bar to higher pressure, because we worked in D_2O instead of H_2O, which has a stabilizing effect[52]), an increase of the MSD value was perceived indicating that this intermediate state corresponds to a much higher flexibility. Due to the large error bars of the MSD values (caused by the high pressure cell thickness induced absorptions) the point at 1750 bar could still be interpreted as deviation within the error limits of the experiment and be in agreement with a gradual decrease up to 3000 bar. However, the difference between the value lying exactly on the slope and the measured point at 1750 bar corresponds to about three times the standard deviation σ (thus $p < 0.05$ according to a t-test, compare Figure 4) so that it is significant. Neutron scattering experiments constitute moreover an average over a huge number of particles, so that the method inherently represents statistical thermodynamics. In reference [15], an onset in loss in activity was observed above 1500 bar indicating the start of denaturation. At higher pressures (between 3 and 6 kbar), the slope of the MSD changed again and the variations in flexibility were less pronounced. This suggests that, in this pressure range, the unfolded state of hAChE U was reached and therefore a reduction of flexibility due to pressure competed with an increase of flexibility due to unfolding. We thus concluded that, for the first time, we measured differences in dynamics between hAChE in its folded state, its high-pressure-induced molten globule state and its unfolded state. This clearly proves that EINS is a sensitive tool

to investigate the pressure dependence of protein conformational fluctuations.

After pressure release, the initial value of the mean square displacement was not recovered (see figure 4), suggesting an irreversible denaturation of hAChE in agreement with earlier determinations of a pressure above 3 kbar necessary for a complete denaturation[15].

Conclusions

In summary, the effect of increasing HHP to human acetylcholinesterase can be described by a four-step model. First at low pressure (1 bar – 1 kbar), the MSD of the hydrogen atoms are only slightly affected. Pressure does not seem to have an impact on the tertiary structure in this pressure range. We conclude that the protein rigidity is strong, but the compression clearly influences the large-scale structure as measured by SANS. Secondly, in the range from 1 – 3 kbar, the global decrease of the MSD reveals that higher pressure reduces significantly the degrees of freedom at the atomic scale due to both Le Châtelier's principle and the reduction of the cavities inside the inner parts of the proteins[53].

We identified a molten globule state at 1750 bar as a third step, since it clearly occurred before unfolding starts. Its signature is a substantial increase of flexibility despite the tendency of pressure to reduce the MSD. In parallel the large scale structure shows an increase of the radius of gyration and the volume which are extended over a broader pressure range. In the fourth step at high pressure (3 – 6 kbar) the protein will face two competitive effects - Le Châtelier's principle reducing the degrees of freedom at the atomic scale on one side, and the unfolding process exposing large hydrophobic parts of the protein to water invading the inner cavities (above 3 kbar[54]) and allowing an increase in the degrees of freedom. This explains the almost linear behavior of the MSD above 3 kbar.

The reversibility of high hydrostatic pressure effects upon proteins is still a debated question. However, during the EINS experiment and after a 6 kbar pressure application the protein showed a decrease in the general MSD indicating irreversibility as the protein loses its functionality being denatured.

The molten globule state is particularly hard to find and corresponds to a very specific pressure range as shown by the change in molecular dynamics probed with EINS. Further experiments such as quasi-elastic neutron scattering (QENS), which furnish more precise information on motion geometry, will help to better characterize this intermediate state dynamically. Thermodynamic investigations of acetylcholinesterase would shed even more light on the facts that lead to the trapping of the protein in a molten globule state since it appears that the type of molten globule depends on the denaturing agent/parameter and can be different for each protein.

Acknowledgements

This work was supported by grants from the Direction Générale de l'Armement (contracts REI no. 2009340023, DGA/SSA 08co501 and BioMedef 0 PDH-2-NRBC-3-C-301). Jérémie Marion was supported by a Ph.D. scholarship from the French Ministry for Research and Technology. We gratefully acknowledge Thomas Gutberlet (HZB), Bruno Demé (ILL), Bernhard Frick (ILL), Moeava Tehei (IHMRI) and Lars Meinhold for fruitful discussions and their technical help. Finally, we thank Mathieu Lemé (ILL) and all members of the SANE group (Jean-Luc Laborier, Claude Payre, Jean-Paul Gonzales, Simon Baudoin, Nadir Belkhier and Eddy Lelièvre-Berna) for their help during the development of the high-pressure equipment. This work benefited from SasView software, originally developed by the DANSE project under NSF award DMR-0520547 [http://www.sasview.org/].

Notes and references

[a] Univ. Grenoble Alpes, IBS, F-38044 Grenoble, France.

[b] Institut Laue Langevin, F-38042 Grenoble Cedex 9, France.

[c] Institut de Recherche Biomédicale des Armées, F-91223 Brétigny sur Orge, France.

[d] Kazan Federal University, Lab of Neuropharmacology, 420008 Kazan, Russian Federation

[e] Angewandte Physikalische Chemie, Universität Heidelberg, 69120 Heidelberg, Germany.

[f] Helmholtz-Zentrum Berlin für Materialien und Energie, 14109 Berlin, Germany.

† These authors contributed equally to this work.

* Corresponding author: J. Peters, email: peters@ill.fr

1 J. Roche, J.A. Caro, D.R. Norberto, P. Barthe, C. Roumestand, J.L. Schlessman, A.E. Garcia, B. García-Moreno E., and C.A. Royer, *Proc Natl Acad Sci U S A*, 1994, **109**, 6945 – 6950.

2 G. Gibrat, G. Hui Bon Hoa, C.T. Craescu, L. Assairi, Y. Blouquit, B. Annighöfer, R.P. May, M.-C. Bellissent-Funel, *BBA – Proteins and Proteomics*, 2014, **1844**, 1560 – 1568.

3 J. Somkuti, M. Bublin, H. Breiteneder and L. Smeller, *Biochem.*, 2012, **51,** 5903−5911.

4 J. Somkuti, Z. Mártonfalvi, M.S.Z. Kellermayer and L. Smeller, *BBA – Proteins and Proteomics*, 2013, **1834**, 112–118.

5 H. Christensen and R. H. Pain, *Eur. Biophys. J.*, 1991, **19**, 221-229.

6 G.V. Semisotnov, N. A. Rodionova, O.I. Razgulyaev, V.N. Uversky, A.F. Gripas and R.I. Gilmanshin, *Biopolymers*, 1991, **31**, 119-128.

7 D.I. Kreimer, R. Szosenfogel, D. Goldfarb, I. Silman and L. Weiner, *Proc Natl Acad Sci U S A*, 1994, **91**, 12145-12149.

8 J. L. Sussman, M. Harel, F. Frolow, C. Oefner, A. Goldman, L. Toker, I. Silman, *Science* 1991, **253**, 872 – 879.

9 S. Darvesh, D.A. Hopkins, C. Geula, *Nat. Rev. Neurosci*., 2003, **4**, 131–138.

10 I. Silman, J.L. Sussman, *Chem. Biol. Interact,*. 2008, **175**, 3–10.

11 E.A. Dolginova, E. Roth, I. Silman and L.M. Weiner, *Biochemistry*, 1992, **31**, 12248-12254.

12 J. Eichler, D. I. Kreimer, L. Varon, I. Silman and L. Weiner, *J Biol Chem*, 1994, **269**, 30093-30096.

13 L. Weiner, D. Kreimer, E. Roth and I. Silman, *Biochem Biophys Res Commun*, 1994, **198**, 915-922.

14 C. Clery, F. Renault, and P. Masson, *FEBS Lett*, 1995, **370**, 212-214.

15 C. Clery-Barraud, A. Ordentlich, H. Grosfeld, A. Shafferman, and P. Masson, *Eur J Biochem*, 2002, **269**, 4297-4307.

16 Y. Kobashigawa, M. Sakurai, K. Nitta, *Protein Sci*., 1999, **8**, 2765-2772.

17 J. Zhang, X. Peng, A. Jones, J. Jonas. *Biochemistry*, 1995, **34**, 8631-8641.

18 G.J.A. Vidugiris, J.L. Markley, C.A. Royer. *Biochemistry*, 1995, **34**, 4909-4912.

19 K. Ruan, R. Lange, N. Bec, C. Balny, *Biochem Biophys. Res. Communic.*, 1997, **239**, 150-154.

20 W. Doster, S. Cusack, W. Petry, *Nature*, 1989, **337**, 754 – 756.

21 G. Zaccai, *Science*, 2000, **288**, 1604-1607.

22 S. Sacquin-Mora, P. Sebban,V. Derrien, B. Frick, R. Lavery, C. Alba-Simionesco, *Biochem.*, 2007, **46**, 14960 – 14968.

23 H. Delacour, S. Lushchekina, I. Mabboux, A.Bousquet, F. Ceppa, L. M. Schopfer, O. Lockridge, P. Masson, PloS One 2014, **9**, e101552.

24 V.F. Sears, *Neutron News*, 1992, **3**, 26−37.

25 F. Gabel, D. Bicout, U. Lehnert, M. Tehei, M. Weik, and G. Zaccai, *Q. Rev. Biophys.,* 2002, **35**, 327-367.
26 M.S. Appavou, G. Gibrat, M-C. Bellissent-Funel, M. Plazanet, J. Pieper, A. Buchsteiner, and B. Annighöfer, *J. Phys.: Condens. Matter*, 2005, **17** 3093 – 3099.
27 M.S. Appavou, S. Busch, W. Doster, A. Gaspar, and T. Unruh, *Eur. Biophys. J.*, 2011, **40**, 705 – 714.
28 J. Peters, M. Trapp, D. Hughes, S.Rowe, B. Demé, J.-L. Laborier, C. Payre, J.-P. Gonzales, S. Baudoin, N. Belkhier and E. Lelievre-Berna, *High Pressure Res.*, 2011, **32**, 97–102.
29 J. P. Hanrahan, M. P. Copley, K. J. Ziegler, T. R. Spalding, M. A. Morris, D. C. Steytler, R. K. Heenan, R. Schweins, and J. D. Holmes, *Langmuir*, 2005, **21**, 4163.
30 J. Peters, M. Trovaslet, M. Trapp, F. Nachon, F. Hill, E. Royer, F. Gabel, L. van Eijck, P. Masson, and M. Tehei, *Phys. Chem. Chem. Phys.,* 2012, **14**, 6764 – 6770.
31 P.K. Glasoe, and F.A. Long, *J. Phys. Chem.*, 1960, **64**, 188-190.
32 T.L. Rosenberry, and D. M. Scoggin, *J Biol Chem*, 1984, **259**, 5643-5652.
33 M.J. Karnovsky, and L.A. Roots, *J. Histochem. Cytochem*., 1964, **12**, 219-221.
34 P. Lindner, and R. Schweins, *Neutron News*, 2010, **21**, 15-18.
35 V. Receveur-Bréchot, and D. Durand, *Curr. Protein Pep. Sc.,* 2012**, 13,** 55-75.
36 A. Guinier, and G. Fournet, Small Angle Scattering of X-rays, 1955, New York.
37 P.V. Konarev, V.V. Volkov, A.V. Sokolova, M.H.J. Koch, and D.I. Svergun, *J. Appl. Cryst.*, 2003, **36**, 1277 - 1282.
38 F. Natali, J. Peters, D. Russo, S. Barbieri, C. Chiapponi, A. Cupane, A. Deriu, M.T. Di Bari, E. Farhi, Y. Gerelli, P. Mariani, A. Paciaroni, C. Rivesseau, G. Schiro, and F. Sonvico, *Neutron News*, 2008, **19**, 14–18.
39 A. Rahman, A., K. S. Singwi, and A. Sjölander, *Physical Review*, 1962, **126**, 986-996.
40 H.H. Paalman, and C. J. Pings*, J. Appl. Phys.,* 1962, **33**, 2635-2639.
41 http://www.ill.eu/instruments-support/computing-forscience/cs-software/all-software/lamp/.
42 S. Bon, M. Huet, M. Lemonnier, F. Rieger, and J. Massoulié, *Eur. J. Biochem.,* 1976, **68**, 523-530.
43 K. Gekko, and H. Noguchi, *The Journal of Physical Chemistry*, 1979, **83**, 2706 – 2714.
44 R.T. Azuah, L. R. Kneller, Y. Qiu, P.L.W. Tregenna-Piggott, C.M. Brown, J.R.D. Copley, and R.M. Dimeo, *J. Res. Natl. Inst. Stan. Technol.*, 2009, **114**, 341.
45 H. Dvir, I. Silman, M. Harel, T.L. Rosenberry, J.L. Sussman, *Chem Biol Interact*, 2010, **187**, 10-22.
46 J. Cheung, M.J. Rudolph, F. Burshteyn, M.S. Cassidy, E.N. Gary, J. Love, M.C. Franklin, and J.J. Height, *J. Med. Chem.*, 2012, **55**, 10282-10286.
47 D.I. Svergun, S. Richard, M.H. Koch, Z. Sayers, *S.* Kuprin, and G. Zaccai, *Proc Natl Acad Sci U S A*, 1998, **95**, 2267-2272.
48 C. Tanford, Physical chemistry of macromolecules, Wiley and Sons Inc, NY, 1961.
49 M. Trapp, M. Trovaslet, F. Nachon, M.M. Koza, L. v. Eijck, F. Hill, M. Weik, P. Masson, M. Tehei, and J. Peters, *J Phys Chem B*, 2012, **116**, 14744 – 14753.
50 M.G. Ortore, F. Spinozzi, P. Mariani, A. Paciaroni, L.R.S. Barbosa, H. Amenitsch, M. Steinhart, J. Ollivier, and D. Russo, *J R Soc Interface*, 2009, **6 Suppl 5**, S619-634.
51 A. Filabozzi, A. Deriu, M. T. Di Bari, D. Russo, S. Croci, and. A. Di Venere, *Biochim Biophys Acta*, 2010, **1804**, 63-67.
52 P. Masson, and C. Balny, *Biochimica et Biophysica Acta*, 1990, **1041**, 223-231.
53 E. Girard, R. Kahn, M. Mezouar, A.C. Dhaussy, T.W. Lin, J.E. Johnson, R. Fourme, *Biophysical Journal*, 2005, **88**, 3562 - 3571.
54 Y. Fu, V. Kasinath, V.R. Moorman, N.V. Nucci, V.J. Hilser, A.J. Wand*, JACS*, 2012, **134**, 8543−8550.